

Study of the internal mechanisms of Pixelized Photon Detectors operated in Geiger-mode

H. Otono^{a,*}, H. Oide^a, S. Yamashita^b, T. Yoshioka^c,
K. Yamamoto^d, K. Yamamura^d, K. Sato^d

^a*Department of Physics, School of Science, The University of Tokyo, 7-3-1 Hongo, Bunkyo-ku, Tokyo 113-0033, Japan*

^b*International Center for Elementary Particle Physics, The University of Tokyo, 7-3-1 Hongo, Bunkyo-ku, Tokyo 113-0033, Japan*

^c*Neutron Science Laboratory, High Energy Accelerator Research Organization (KEK), 1-1 Oho, Tsukuba, Ibaraki 305-0801, Japan*

^d*Solid State Division, Hamamatsu Photonics K.K., 1126-1 Ichino, Higashi-ku, Hamamatsu, Shizuoka 435-8558, Japan*

Abstract

In the 1990s, a novel semiconductor photon-sensor operated in Geiger-mode was invented in Russia (Silicon PhotoMultiplier), which consists of many tiny pixels and has a single photon level sensitivity. Since then, various types of the sensor with this scheme, Pixelized Photon Detectors (PPD), have been developed in many places in the world. For instance, Hamamatsu Photonics K.K. in Japan produces the PPD as a Multi-Pixel Photon Counter.

While the internal mechanisms of the PPD have been intensively studied in recent years, the existing models do not succeeded to fully reproduce the output characteristic, such as waveforms at low temperature. We have developed a new model with the transient multiplication and quenching of the realistic avalanche process and have succeeded in reproducing the output waveform of the PPD at various temperature. In this paper, we discuss our improved model.

Key words: PPD, Multi-Pixel Photon Counter, Silicon PhotoMultiplier, Internal mechanism, SiPM, MPPC

1. Introduction

In the 1990s, a novel semiconductor photon-sensor operated in Geiger-mode was invented in Russia (Silicon PhotoMultiplier) [1, 2], which consists of many tiny pixels and has a single photon level sensitivity. Since then, various types of the sensor with this scheme have been developed in many places in the world [3]. For instance, Hamamatsu Photonics K.K. (HPK) in Japan produces a Multi-Pixel Photon Counter (MPPC) [4, 5]. Recently these devices are called as Pixelized Photon Detectors (PPD) [6].

Since the PPD has many advantages over PMTs, such as compact size, low cost, low power consumption and insensitive to magnetic field, it could be a successor to them in high energy experiments and/or in medical fields in the near future.

The particular device studied in this paper is S10262-11-025 of MPPC by HPK which has a 1mm × 1mm photosensitive surface and consists of 1600 pixels in total.

We studied the basic properties of the MPPC at low temperature [7] and found that output waveform has a spike component which can not be fully explained by existing models. We introduced a new model in which the realistic avalanche process is considered and succeeded in reproducing the output waveform at various temperature.

* corresponding author.

Email address: otono@icepp.s.u-tokyo.ac.jp
(H. Otono).

2. Existing models of the PPD

2.1. The traditional model

Figure 1 shows the traditionally used equivalent circuit for the PPD which explains the linearity between the gain (G) and the operating voltage (V_{op}). The PPD has multiple pixels and each pixel consists of a diode and a quenching resistor (R_q). The PPD is operated at a few volts higher than the breakdown voltage (V_{br}), namely Geiger-mode, and the diode itself does not have the capability to terminate the avalanche process. Hence, the quenching resistor is necessary in order to decrease the voltage applied to the diode. When the current fed into the resistor is $I_{expected} \equiv \frac{\Delta V}{R_q}$, where ΔV is $V_{op} - V_{br}$, the voltage applied to the diode drops to V_{br} and the multiplication stops. As a result, the gain is obtained as follows: $G = \frac{C_d \times \Delta V}{e}$, where C_d is the capacitance value of the diode and e the elementary electric charge.

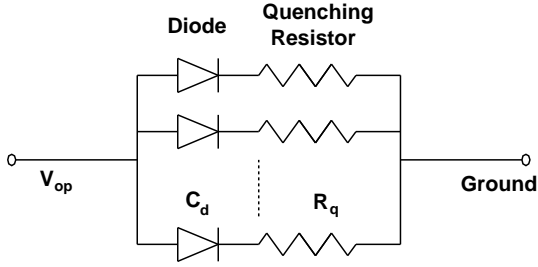


Fig. 1. A simple circuit of the PPD. Each pixel consists of a diode and a quenching resistor.

2.2. Waveform at low temperature

We studied the basic properties, such as waveforms, of MPPC produced by HPK at 300K, 200K and 77K [7]. The used amplifier was C5549 (bandwidth 1.5GHz) produced by HPK whose multiplication factor and input impedance are 63 and 50Ω , respectively. Figure 2 shows the average waveform at each temperature, where ΔV is fixed at 3.0V, and a spike component is seen in the waveforms taken at 200K and 77K. Although the existence of two components has already been reported by the ITC-irst group at room temperature with a SiPM [8, 9], it is the first time to observe the sharp spike component shown in the waveform of MPPC at 77K.

R_q can be measured from the forward current-voltage characteristics of the PPD by using the

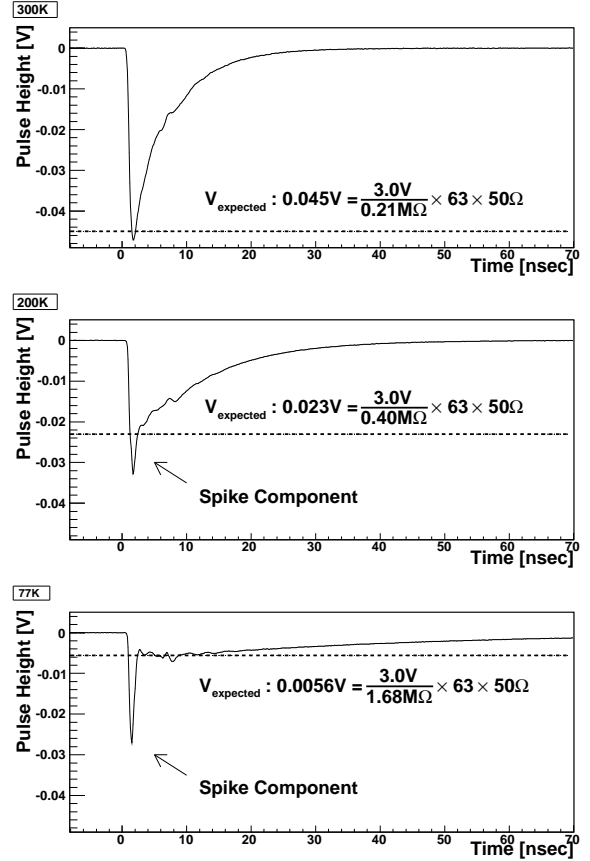


Fig. 2. Waveforms observed at 300K (top), 200K (middle) and 77K (bottom). The waveforms at 200K and 77K have two components.

following equation: $\frac{R_q}{N_{pixels}} = \frac{V_f}{I_f}$, where I_f, V_f and N_{pixels} are the forward current value, the forward voltage and the number of pixels, respectively. The resistor values obtained were shown in Table 1.

The negative temperature coefficient of resistivity is due to the amorphous-like structure of poly-silicon [10] which is the main component of the quenching resistor in the MPPC.

2.3. A problem on the traditional model

Dashed lines in the Figure 2 indicate the expected pulse height ($V_{expected}$) by the traditional model, which can be obtained from the following equation: $V_{expected} = I_{expected} \times A \times Z_{input}$, where A is the multiplication factor of the amplifier and Z_{input} is the input impedance.

The spike component becomes much higher than $V_{expected}$ at low temperature. The traditional model is thus not sufficient for explaining the output wave-

form of the PPD. V_{expected} and the measured pulse height (V_{measured}) at each temperature are also summarized in Table 1.

T [K]	R_q [M Ω]	V_{expected} [V]	V_{measured} [V]
300	0.21	0.045	0.047
200	0.40	0.023	0.033
77	1.68	0.0056	0.027

Table 1
 R_q , V_{expected} and V_{measured} at each temperature.

2.4. A model developed by the ITC-irst group

ITC-irst group looked into a capacitance (C_q) located between the quenching resistor and the diode as a possible reason for explaining two components. C_q is typically in the order of 1fF [11]. Figure 3 shows its equivalent circuit proposed by them. They simplified the scheme of the multiplication and quenching and substituted a switch. R_s is the series resistance of the diode.

As a consequence, they succeeded in reproducing the two components by tuning the parameters, such as R_s and C_q .

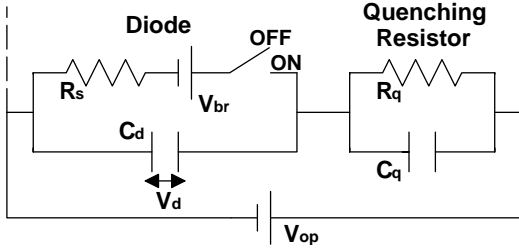


Fig. 3. An equivalent circuit of a single pixel which was developed by the ITC-irst group [8, 9].

3. A new model including the avalanche process

Although the existence of the two components is explained by ITC-irst group, the avalanche process is described by the switch and the transient multiplication is not included in their model. We introduce a new model in which the realistic avalanche process is considered so as to reproduce well the output waveform.

3.1. A reproduction of the output waveforms

Our model is shown in Figure 4 and it is described by the charge of created carriers $q(t)$ in the multiplication layer in the diode rather than by the switches of the model by ITC-irst group.

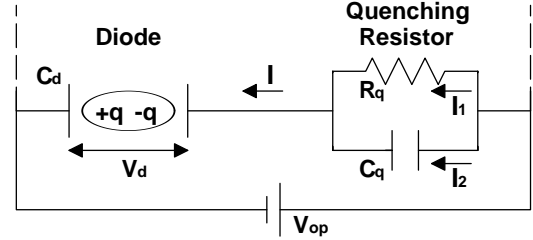


Fig. 4. A new equivalent circuit proposed in this paper.

$\frac{dq(t)}{dt}$ depends on the ionization rate of electrons and holes, α_e and α_h , which are proportional to $E(x) \exp(-\frac{B}{E(x)})$, where $E(x)$ is the electric field strength and B is a constant [12]. We calculated the ionization rate from the interpolated values of the measurement by Grant [13]. Thus $\frac{dq(t)}{dt}$ can be expressed by:

$$\begin{cases} \frac{dq(t)}{dt} = \sum_{i=e,h} \int_0^L e \rho_{i(x)} \alpha_{i(E(x))} v_{i(E(x))} dx^3 \\ V_d(t) = \int_0^L E(x) dx, \end{cases}$$

where ρ_e and ρ_h are the densities of electrons and holes in the diode, v_e and v_h are the drift velocities of each carrier, $V_d(t)$ is the voltage applied to the diode and L is the width of the diode. In this calculation, L is fixed at $2\mu m$.

We fixed v_e and v_h at $v = 1 \times 10^7$ cm/sec, because they are saturated and remain constant in the high electric field at any temperature [14], and ignored the temperature dependence of α_e and α_h [15]. We calculated the electric field of the typical PPD [16] and obtained the almost uniform electric field in the multiplication layer in the diode, thus we substitute $\alpha_{(V_d(t))}$ for $\alpha_{(E(t))}$. As a result, the equations are simplified as follows:

$$\frac{dq(t)}{dt} = ev \sum_{i=e,h} \int \rho_{i(x)} \alpha_{i(V_d(t))} dx^3. \quad (1)$$

Next, the circuit equations are the following:

$$\begin{cases} I = I_1 + I_2 \\ V_{op} = V_d(t) + I_1 R_q \\ V_{op} = V_d(t) + \frac{\int_0^t I_2 dt}{C_q}, \end{cases}$$

where I is the observable current. The equation of equilibrium of the charge in the diode is calculated from $q(t)$ and $I(t)$:

$$C_d \frac{dV_d(t)}{dt} = \frac{dq(t)}{dt} - I(t).$$

I_1 , I_2 and I are substituted into the first equation and the following differential equation can be obtained:

$$\frac{dV_d(t)}{dt} = \frac{1}{R_q(C_d + C_q)} (V_{op} - V_d(t) - R_q \frac{dq(t)}{dt}). \quad (2)$$

From Eqs.(1) and (2), $V_d(t)$ and $q(t)$ are sequentially solved and the output current of the PPD can be expressed by:

$$I(t) = C_d \frac{dV_d(t)}{dt} + \frac{dq(t)}{dt}.$$

For the purpose of comparison with observed current, the frequency characteristics of the used connectors, cables and amplifier have to be taken into account [17]. For our system the transmission properties are determined by the connector since it has the smallest bandwidth of all components at 1.4GHz (Suhner QLA). The bandwidths of the amplifier and the cable are 1.5GHz and 2.0GHz, respectively. Figure 5 shows the pulse distortion of our system.

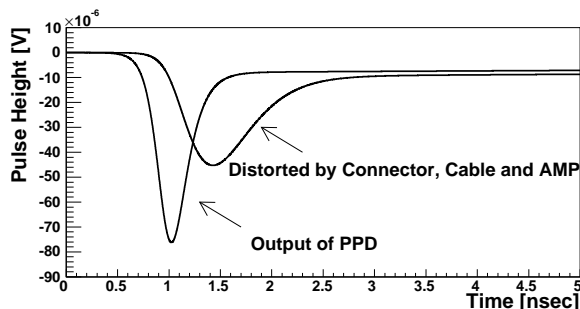


Fig. 5. Expected output of the PPD and the distortion due to connectors, cables and an amplifier.

Hence, the leading and trailing edge of the spike component at 77K are characterized by the bandwidth of the connector, 1.4GHz. R_q is already obtained as 1.68M Ω and C_d can be calculated from the time constant of the recovery process, $R_q C_d$ [18]. In

order to calibrate C_q , we evaluate the pulse height of spike component at 77K, because it is the most sensitive to the variation of C_q . Consequently, we can obtain C_q as 2fF.

The expected and measured waveforms at each temperature are shown in Figure 6 by the solid and dashed curves, respectively. All parameters are summarized in Table 2. Note that C_d and C_q are calibrated from the waveform at 77K. The same values are applied to the waveform at 200K and 300K.

T [K]	R_q [M Ω]	C_d [fF]	C_q [fF]
77	1.68	20.2	2
300	0.21	20.2	2
200	0.40	20.2	2

Table 2

R_q at each temperature is measured value. C_d and C_q are calibrated from waveform at 77K. The same values are applied to the waveform at 200K and 300K.

The waveforms in Figure 6 are the closeup view of Figure 2 and the expected waveforms compare well with the measured ones. Therefore, our model properly includes the multiplication and quenching process and reproduces the output waveform of the PPD.

3.2. A reproduction of $G - \Delta V$ relationship

In the model by ITC-first group, the linearity between the gain of the PPD (G) and ΔV is determined by the opening of the switch when V_d drops to V_{br} , which forces the termination of the avalanche process. This guarantees that the gain relationship is in accord with PPD measurements, for which the relationship is indeed linear. In our model there is no such forcing, and as such V_d drops below V_{br} . Thus, this linearity is not trivially determined. We have though calculated the $G - \Delta V$ relationship from the model and have in fact found it to be linear as shown in Figure 7 which is further verification of the model.

4. Conclusion

We developed a new model for a Pixelized Photon Detector (PPD), which includes the dynamical avalanche process. By calculating the circuit equations of the model, the multiplication and quenching process can be naturally incorporated as following.

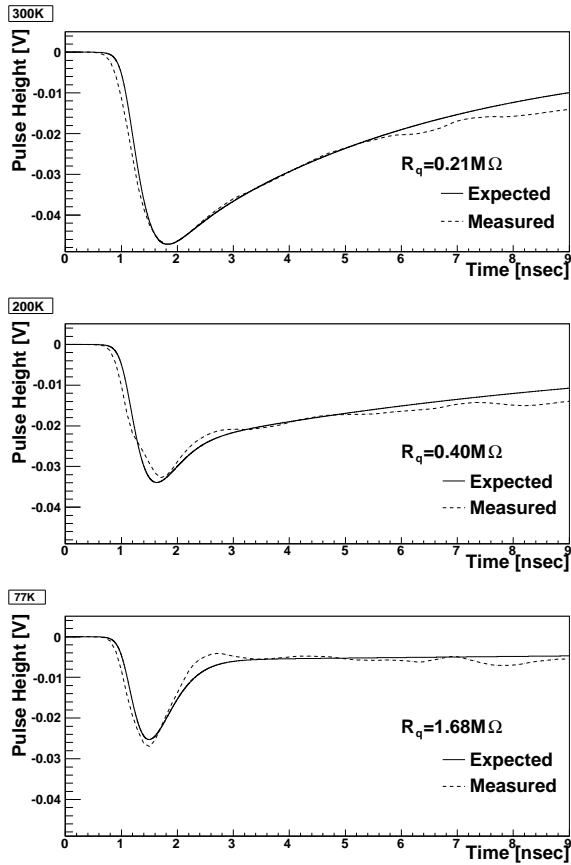


Fig. 6. Closeup view of Figure 2. The waveform expected from our proposed model and the measured waveform.

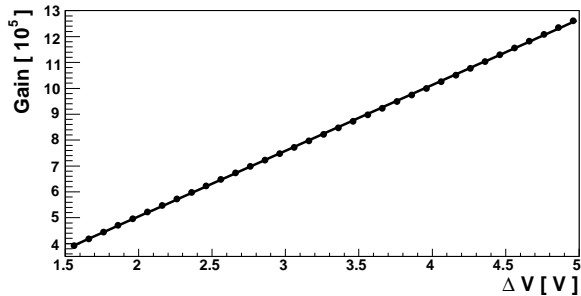


Fig. 7. The linearity between the gain and the operation voltage, which is calculated from our model.

The moment the avalanche process occurs, the current feeds into the capacitance C_q and is observed as the spike component of the waveform. The leading and trailing edge of the spike component is determined by the transmission properties of the measurement system. At the same time, the avalanche multiplication begins to be suppressed by the current fed into the quenching resistor R_q and finally

quenches. After quenching, the recovery process is characterized by the time constant, $R_q C_d$, where C_d is the capacitance value of the diode.

Furthermore we have succeeded in reproducing the observed characteristic waveforms, such as sharp spike component at 77K. The waveforms at 200K and 300K can also reproduced with C_d and C_q calibrated from the waveform at 77K and measured R_q . Note that there is no variable for reproducing the waveforms at 200K and 300K.

Consequently, the model proposed in this paper makes it possible to properly incorporate the internal mechanisms of the PPD. Therefore, it should play an important role for the development of PPDs in the future.

5. Acknowledgments

The authors wish to express our deep appreciation to the KEK-DTP photon-sensor group members for their helpful discussions and suggestions. This work was supported by Grant-in-Aid for JSPS Fellows 20-4439 and by Grant-in-Aid for Exploratory Research 20654021 from the Japan Society for the Promotion of Science (JSPS).

References

- [1] V. Golovin. *Patent No. RU*, 2142175, 1998.
- [2] Z. Sadygov. *Patent No. RU*, 2102820, 1998.
- [3] D. Renker. Geiger-mode avalanche photodiodes, history, properties and problems. *Nucl. Instr. Meth.*, A567:48–56, 2006.
- [4] K. Yamamoto et al. Newly developed semiconductor detectors by Hamamatsu. *Proceedings of International Workshop on new Photon-Detectors PD07*, PoS(PD07)004.
- [5] S. Gomi et al. Development and study of the multi pixel photon counter. *Nucl. Instr. Meth.*, A581:427–432, 2007.
- [6] C. Amsler et al. Review of particle physics. *Phys. Lett.*, B667:1, 2008.
- [7] H. Otono et al. Study of MPPC at liquid nitrogen temperature. *Proceedings of International Workshop on new Photon-Detectors PD07*, PoS(PD07)007.
- [8] C. Piemonte et al. Characterization of the First Prototypes of Silicon Photomultiplier Fabricated at ITC-irst. *IEEE Transaction on Nuclear Science*, Vol.54, No.1:236–244, 2007.

- [9] C. Piemonte et al. A New Silicon Photomultiplier structure for blue light detection. *Nucl. Instr. Meth.*, A568:224–232, 2006.
- [10] K. Kato et al. A Physical Mechanism of Current-Induced Resistance Decrease in Heavily Doped Polysilicon Resistors. *IEEE Trans. Elec.*, ED-29, No.8:1156–1161, 1982.
- [11] F. Corsi et al. Modeling a silicon photomultipliers (SiPM) as a single source for optimum front-end design. *Nucl. Instr. Meth.*, A572:416–418, 2007.
- [12] W. Maes et al. Impact Ionization in Silicon: A Review and Update. *Solid-State Electronics*, Vol.33, No.6:705–718, 1990.
- [13] W.N. Grant. Electron and hole ionization rates in epitaxial silicon at high electric fields. *Solid-State Electronics*, Vol.16:1189–1203, 1973.
- [14] C. Jacobi et al. A review of some charge transport properties of silicon. *Solid-State Electronics*, Vol.20:77–89, 1977.
- [15] K. Rose et al. Temperature dependent effective ionization coefficient for Si. *J. Appl. Phys.*, Vol.83, No.9:4988–4990, 1998.
- [16] T. Kagawa et al. Design of Deep Guard Ring for Geiger Mode Operation Avalanche Photodiode. *IEICE TRANS. ELECTRON.*, Vol.E88-CC, No.11, 2005.
- [17] G Brianti. Distortion of Fast Pulses in Coaxial Cables Numerical Analysis and Applications. *Cern Yellow Report*, 65-10, 1965.
- [18] H. Oide et al. Study of afterpulsing of MPPC with waveform analysis. *Proceedings of International Workshop on new Photon-Detectors PD07*, PoS(PD07)008.